Research Square

Preprints are preliminary reports that have not undergone peer review.
They should not be considered conclusive, used to inform clinical practice,
or referenced by the media as validated information.

Muscovite chemistry records contrasting fractionation trends in zoned pegmatites from the Seridó Pegmatite Province, northeastern Brazil

Luciano Schaefer Pereira

luciano.pereira@ifpb.edu.br

Instituto Federal de Educação Ciência e Tecnologia da Paraíba

Marcos Antônio Leite Nascimento

Universidade Federal do Rio Grande do Norte

Research Article

Keywords: Muscovite, Granitic pegmatites, Magmatic fractionation, Tantalum, Element decoupling.

Posted Date: November 25th, 2026

DOI: https://doi.org/10.21203/rs.3.rs-11258036/v1

License: This work is licensed under a Creative Commons Attribution 4.0 International License.
Read Full License

Additional Declarations: No competing interests reported.

Muscovite chemistry records contrasting fractionation trends in zoned pegmatites from the Seridó Pegmatite Province, northeastern Brazil

Luciano Schaefer Pereira [a],*, Marcos Antônio Leite do Nascimento [b]

a Instituto Federal de Educação, Ciência e Tecnologia da Paraíba (IFPB), Campus João Pessoa, Av. Primeiro de Maio, 720, Jaguaribe, 58015-435, João Pessoa, PB, Brazil

b Departamento de Geologia, Universidade Federal do Rio Grande do Norte (UFRN), Campus Universitário Lagoa Nova, Av. Senador Salgado Filho, s/n, 59078-970, Natal, RN, Brazil

* Corresponding author. E-mail address: luciano.pereira@ifpb.edu.br

Abstract

Muscovite is the only K-bearing phase present across all crystallisation stages of many granitic pegmatites, and its chemistry therefore offers a continuous record of magmatic evolution. We use 64 muscovite spot analyses (electron microprobe and LA-ICP-MS) from the internal zones of two zoned LCT pegmatites of the Seridó Pegmatite Province, northeastern Brazil, to test whether the two bodies followed a common fractionation trajectory. In both pegmatites the K/Rb, K/Cs and Al/Ga ratios decrease systematically from margin to core, and Rb and Cs increase together, defining a convergent alkali-fractionation trend. The high-field-strength elements, however, behave differently: Mamões evolves towards strong Ta enrichment and progressively lower Nb/Ta, whereas Capoeira 1 advances mainly in caesium, with only modest Ta gain and comparatively high Nb/Ta. Fluorine rises markedly at Mamões but not at Capoeira 1, mirroring the divergence in Ta. Euhedral muscovite booklets, restricted to Mamões, are distinguished from replacement-body micas by their habit and by an order-of-magnitude lower compositional dispersion, and are interpreted, together with petrographic relationships and Li/Rb systematics, as primary magmatic muscovite. These results show that muscovite does not record a single fractionation path in the Seridó Pegmatite Province: alkali enrichment is convergent, but Ta–Nb evolution becomes decoupled between the two bodies, with Ta enrichment at Mamões contrasting with the Cs-dominated evolution of Capoeira 1.

Keywords: Muscovite; Granitic pegmatites; Magmatic fractionation; Tantalum; Element decoupling.

1. Introduction

The region known as the Seridó Pegmatitic Province, located within the Seridó UNESCO Global Geopark (or simply Seridó Geopark), is one of the most extensive pegmatite-bearing areas in the whole of South America and also one of the main global suppliers of minerals such as tantalum and beryllium (Johnston Jr. 1945; Beurlen et al. 2014). This territory hosts thousands of pegmatite bodies, which can be classified into two main groups: those of homogeneous composition and those with zoned (heterogeneous) structures.

The former display constant texture, contain no significant concentrations of metallic minerals and differ from pegmatitic granites in occurring as dykes with a discordant orientation relative to the neighbouring rocks. Pegmatitic granites, in turn, appear as intrusive masses of the *stock* or sill type, are peraluminous and exhibit large to enormous crystals (Sales 2020).

Heterogeneous bodies, in turn, are marked by a well-defined internal compartmentalisation — including marginal zones (zone I), walls (zone II), intermediate bands (zone III) and quartz cores (zone IV), as well as mineral replacement areas (between zones III and IV) — and occur as dykes, being the main hosts of elements such as tantalum, niobium, beryllium, tin and lithium (Johnston Jr. 1945; Da Silva et al. 1995).

These pegmatite bodies are the end products of the differentiation of granitic magmas, whose late crystallisation and volatile enrichment favour the concentration of incompatible elements, such as rare metals (London 2008). The investigation of micas — especially muscovite, the main mica type occurring in all pegmatites and, to a lesser degree, in pegmatitic granites — has proved an effective tool for evaluating the degree of fractionation of pegmatitic systems and inferring their mineralogical potential, because this mineral occurs throughout all crystallisation stages and records systematic compositional variations along the evolutionary process (Černý et al. 1985).

On this basis, we test whether muscovite chemistry records a common fractionation trajectory in two zoned pegmatites of the Seridó Pegmatite Province, and whether the behaviour of Ta and Nb relative to Rb and Cs can discriminate distinct evolutionary pathways and possible magmatic–hydrothermal overprints. To this end, 64 muscovite spot analyses were obtained from the border, wall and replacement-body zones of the Mamões and Capoeira 1 pegmatites, together with the euhedral muscovite booklets from the contact between zones III and IV in the Mamões pegmatite.

2. Geological setting

The Seridó Geopark lies within the Borborema Province, characterised by a fold system developed during the Brasiliano/Pan-African Cycle (Almeida et al. 1981), related to the Gondwana amalgamation process, which includes Archean, Palaeoproterozoic and Mesoproterozoic nuclei affected by transpressive tectonics and marked by structural lineaments, the Patos Lineament being the main one, together with tight folds.

The mapped area lies in northeastern Brazil, in the state of Rio Grande do Norte, 250 km west of the municipality of Natal. The study area, inside the Seridó Geopark, covers about 150 km² and is delimited by the coordinates 6°35′S–7°00′S and 36°30′W–36°47′W, forming an irregular polygon that encompasses the towns of Carnaúba dos Dantas, Equador, Parelhas and Santana do Seridó.

The region can be accessed from Natal via highways BR-101 and BR-226 to the town of Acari and via road RN-11, which links Parelhas (RN) to Equador (PB), towards Santa Luzia (PB). All roads are paved and asphalted and in good driving conditions.

The Geopark territory is located in the Rio Piranhas–Seridó Domain, composed of Palaeoproterozoic orthogneisses of the Caicó Complex in the basement (Fig. 1), corresponding to about 2 % of the territory. Discordantly overlying the Caicó Complex, the Seridó Group is a Neoproterozoic metavolcano-sedimentary sequence composed of paragneisses, quartzites and marbles of the Jucurutu Formation at the base, followed by quartzites and metaconglomerates of the Equador Formation, and by schists of varying metamorphic grade of the Seridó Formation at the top. The Seridó Group corresponds to 69.47 % of the total area. Also of Neoproterozoic age are the granites of the Dona Inês and Itaporanga Intrusive Suites, as well as the diorites/gabbros of the São João do Sabugi Intrusive Suite, comprising 21.26 % of the territory. Pegmatite dykes/bodies occur throughout the region, mainly emplaced in the mica schists of the Seridó Formation. Meso-Cenozoic magmatism is represented in the area by diabase and basalt of the Rio Ceará-Mirim Volcanism and basalts of the Macau Volcanism. Pegmatite, diabase and basalt have limited territorial expression. Finally, the conglomerates and sandstones of the Serra do Martins Formation constitute the Cenozoic cover of the area, corresponding to 7.25 % of the local unit. Old and recent alluvial deposits are the youngest geological units.

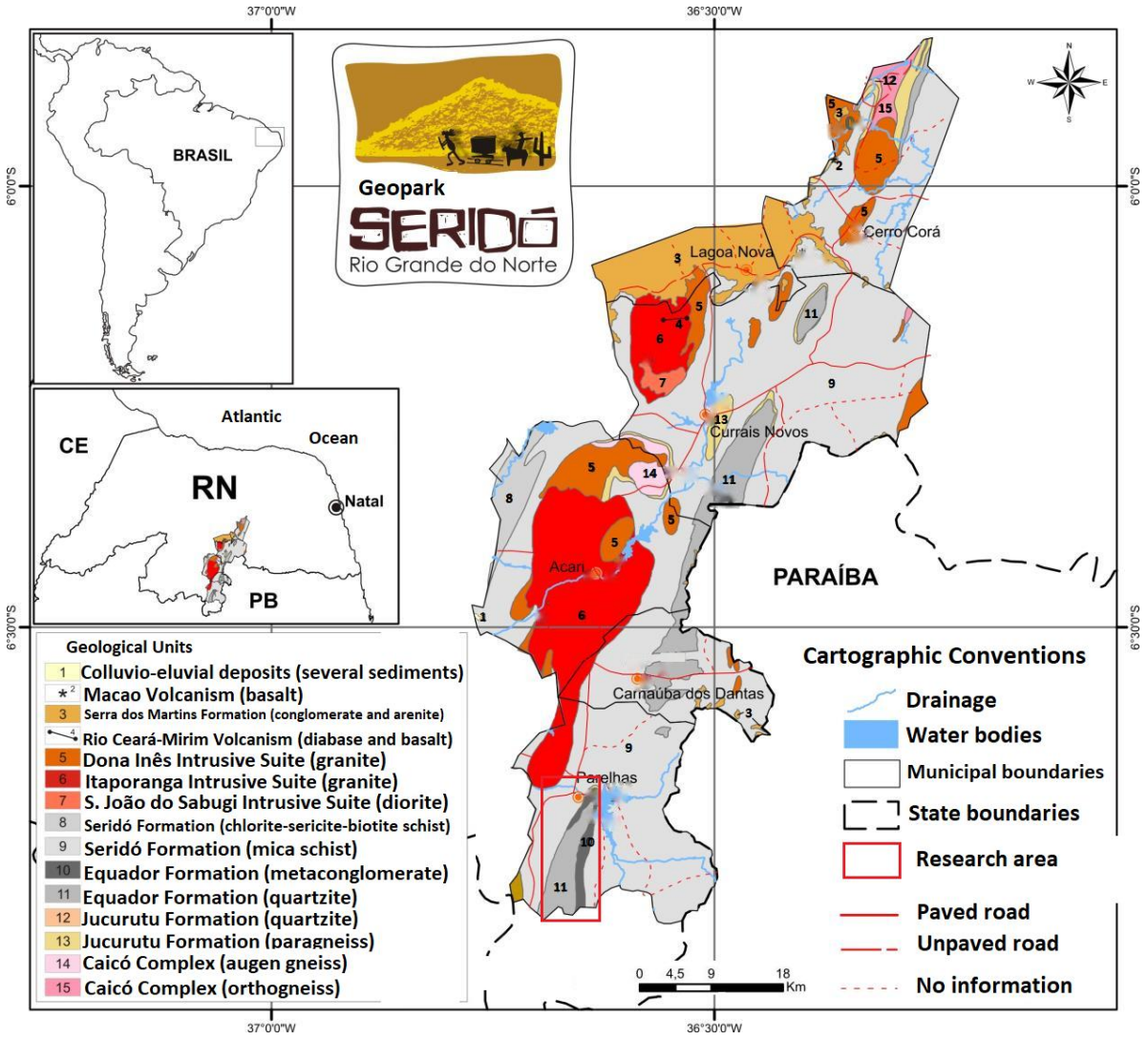

Fig. 1 Geological map of the Seridó UNESCO Global Geopark with the delimitation of the study area (in red). Source: modified from Nascimento (2018).

2.1. The Borborema Pegmatite Province

Scorza (1944) proposed the term "Borborema Pegmatite Province" to identify the region of northeastern Brazil where pegmatites are widespread, spanning areas in the states of Paraíba and Rio Grande do Norte. This designation was later updated to "Seridó Pegmatite Province", owing to its predominance within the geological limits of the Seridó Belt (Santos et al. 2014).

Geologically, the region is part of the Seridó Belt, a Neoproterozoic metamorphic belt belonging to the Borborema Province. This belt is composed of metasedimentary rocks (paragneisses, marbles, calc-silicate rocks, quartzites, metaconglomerates and mica schists) and of syn- to late-tectonic granites, and is marked by shear zones that control the intrusion of pegmatite bodies.

The Seridó pegmatites became known in the early twentieth century, when they began to be exploited for mica extraction, particularly around the end of the First World War. With the outbreak of the Second World War and the consequent increase in demand for strategic minerals such as niobium, tantalum and beryllium, mining activity in the area was significantly expanded (Da Silva 1993). During that period, more than 450 pegmatite bodies were exploited, contributing approximately 20 % of global tantalite production and 10 % of beryl (Rolff 1945). It was also in this context that pioneering studies on the region's pegmatites emerged, conducted by researchers such as Scorza (1944) and Rolff (1945).

The pegmatites of the region crop out as discordant dykes of varied geometry (tabular, lenticular, irregular), with dimensions ranging from a few metres up to 600 m long by 50 m wide. Their intrusion occurs preferentially in the quartzites and metaconglomerates of the Equador Formation and in the mica schists of the Seridó Formation, and many show a genetic relationship with the Parelhas Pegmatoid Granite (Pereira 2000), a peraluminous intrusive body of vein-like orientation, about 6 × 1.5 km in extent. The western limit of this granite is marked by the Serra dos Quintos Shear Zone (Fig. 2).

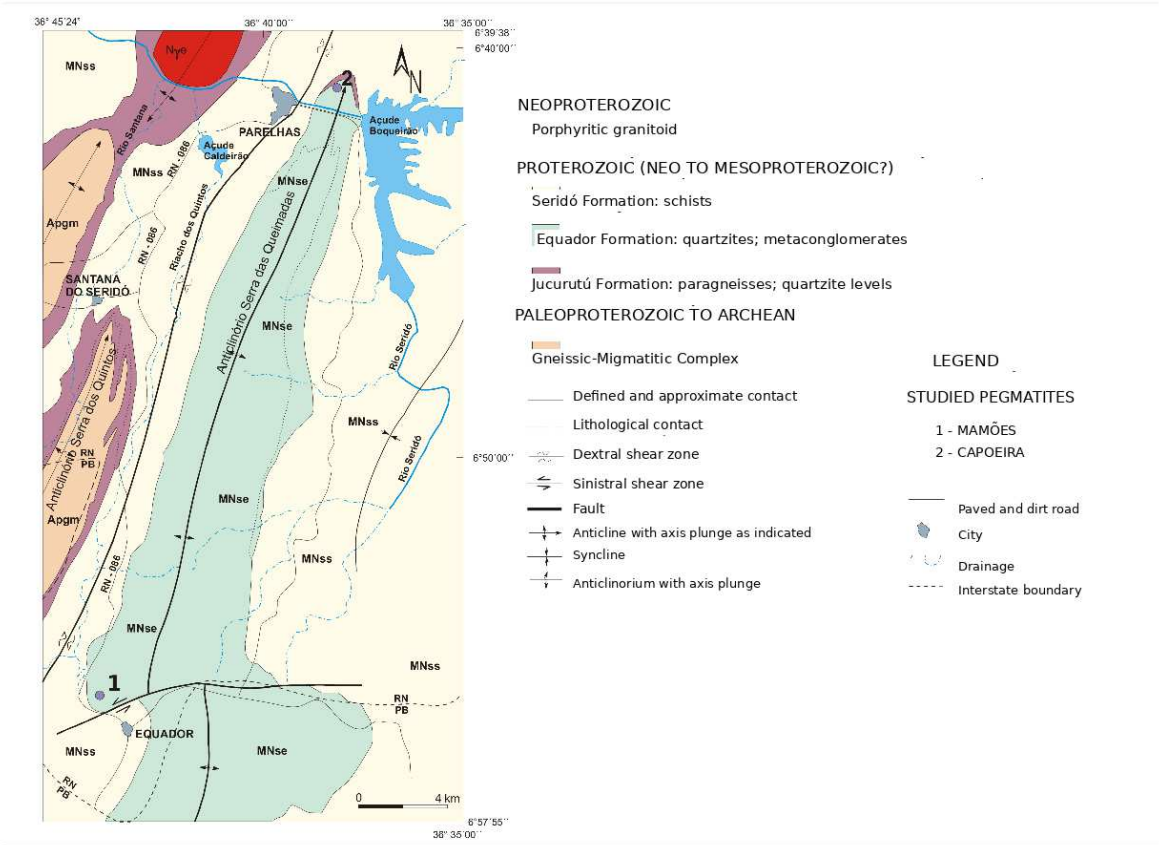

Fig. 2 Geological map of the Borborema Pegmatite Province, with the delimitation of the mapped pegmatites. Source: modified from Moraes (1999).

The pegmatite dykes cropping out in the area can be subdivided into three classes: homogeneous (simple, unzoned and poorly to non-mineralized), heterogeneous (complex, zoned and mineralized) and mixed.
These pegmatites have shapes that tend to vary according to the host rock, and may be lenticular, tabular or circular, without ruling out branched to irregular forms; they are best preserved when they intrude quartzites and metaconglomerates, owing to the competence of the host rock.
These pegmatites have dimensions ranging from 50–80 m long by 3 m wide to 600 m long by 50 m wide (as is the case of the sampled pegmatites, Fig. 3), and their zonation was proposed by Johnston Jr. (1945), as follows:

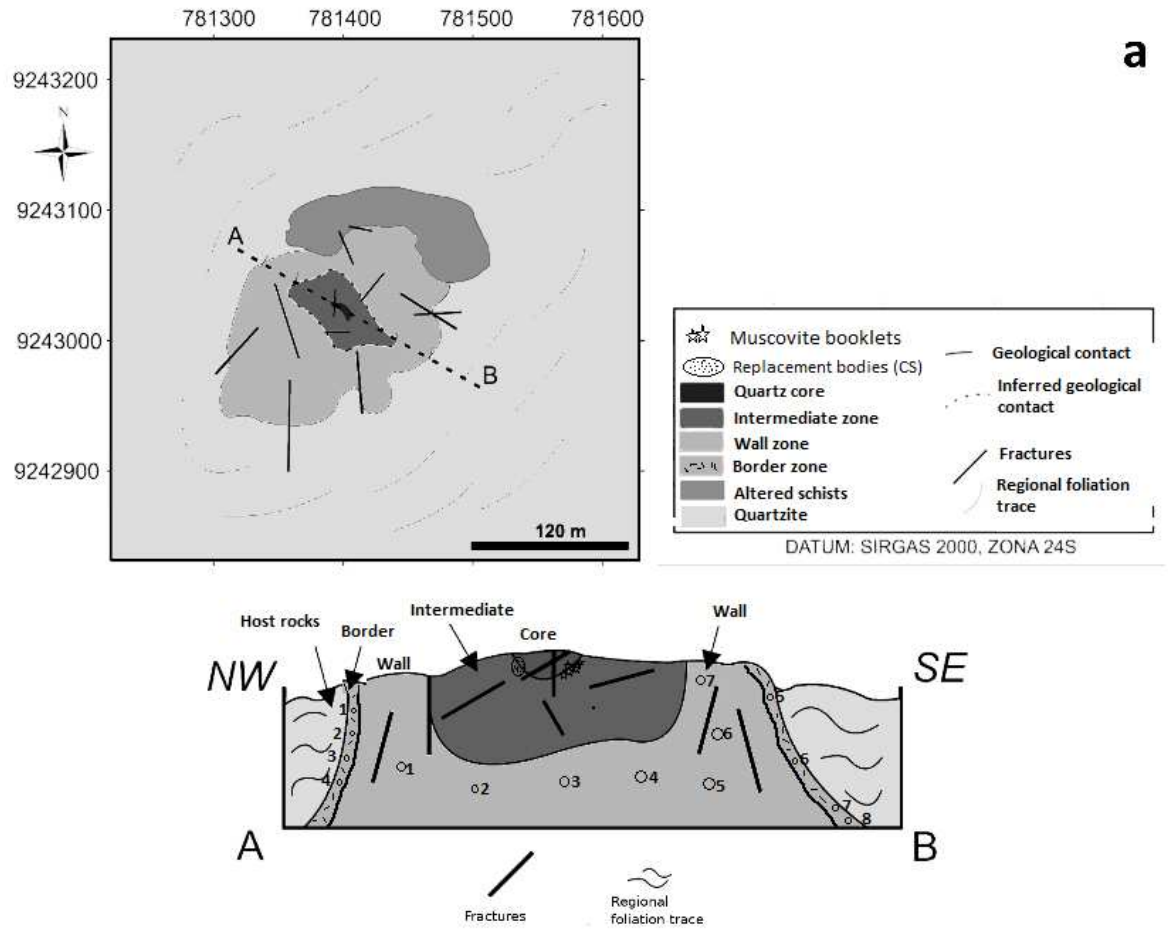
a
781300
781400
781500
781600
9243200
9243100
9243000
9242900
A
B
120 m
Muscovite booklets
Replacement bodies (CS)
Quartz core
Intermediate zone
Wall zone
Border zone
Altered schists
Quartzite
Geological contact
Inferred geological contact
Fractures
Regional foliation trace
DATUM: SIRGAS 2000, ZONA 24S
Host rocks
Border
Intermediate
Core
Wall
Wall
NW
SE
A
B
Fractures
Regional foliation trace

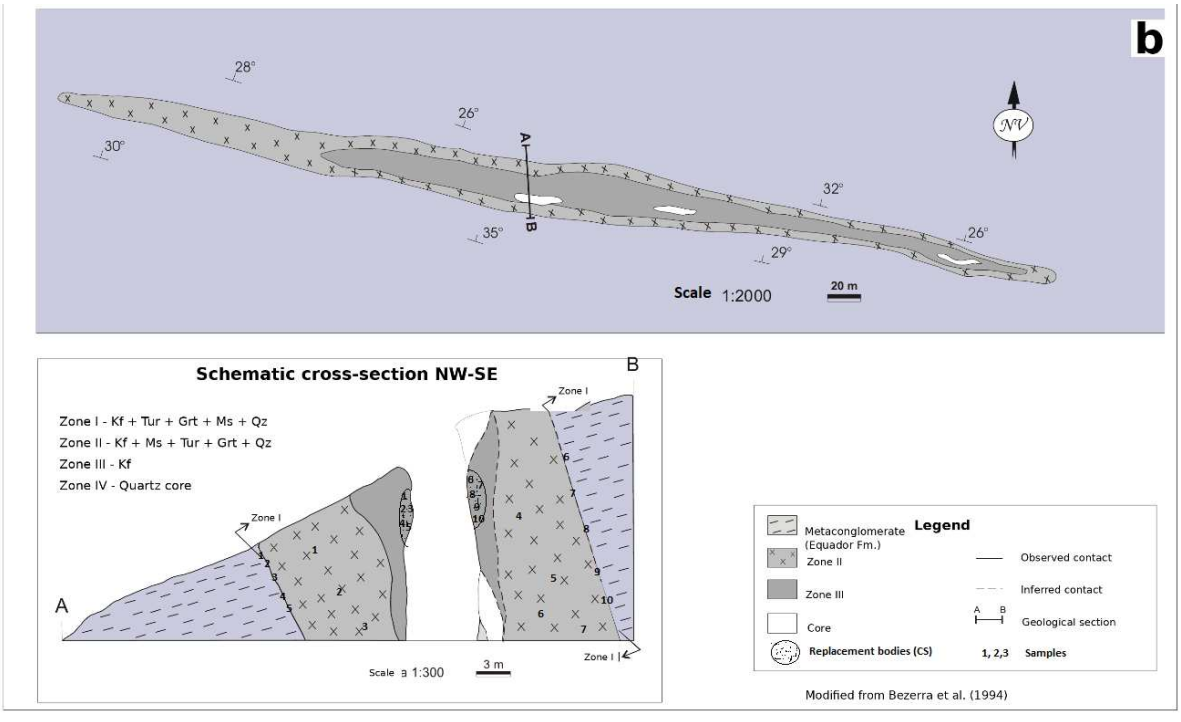
b
28°
26°
30°
32°
35°
29°
26°
A
B
NV
Scale 1:2000
20 m
Schematic cross-section NW-SE
Zone I - Kf + Tur + Grt + Ms + Qz
Zone II - Kf + Ms + Tur + Grt + Qz
Zone III - Kf
Zone IV - Quartz core
Zone I
Zone I
Zone I
A
B
Scale a 1:300
3 m
Legend
Metaconglomerate (Equador Fm.)
Zone II
Zone III
Core
Replacement bodies (CS)
Observed contact
Inferred contact
Geological section
1, 2,3 Samples
Modified from Bezerra et al. (1994)

Fig. 3 Profiles of the sampled pegmatites with their respective zones. (a) Mamões (source: Pereira 2000); (b) Capoeira 1. Numbers 1, 2,3… represents the samples. (source: modified from Bezerra et al. 1994).

Zone I (border zone): corresponds to the contact zone with the host rock, of centimetric to decimetric size. It occurs mainly in pegmatites that cut mica schists, has an aplitic texture and is composed of albite and quartz, centimetric crystals of muscovite and tourmaline (dravite type) and millimetric crystals of garnet. In the Mamões pegmatite this zone is about 10 cm thick, with muscovite crystals growing perpendicular to the contact with the host rock, resulting in a texture known as *cockscomb*, whereas in the Capoeira pegmatite this zone consists essentially of tourmaline crystals (Fig. 4a).

Zone II (wall zone): the transition from zone I to zone II may be gradational or sharp, and is texturally and mineralogically similar to homogeneous pegmatites, being tens of metres wide (Fig. 4b). It is composed of microcline megacrysts with regular lamellar perthite, intergrown with quartz in graphic texture. Its coarse interstitial assemblage consists essentially of quartz, feldspar, muscovite, tourmaline and garnet and, more rarely, biotite. The regular lamellar perthite of the microcline, attributed to subsolidus exsolution, and the graphic intergrowth with quartz, indicative of cotectic crystallisation from a supersaturated liquid, together with the crystalline gigantism and the absence of replacement features, characterise this zone — like zone I — as the product of essentially magmatic crystallisation, corresponding to the main solidification volume of the pegmatitic melt.

Zone III (intermediate zone): the transition from zone II to zone III is gradational. Its characteristic mineral is perthitic microcline, which reaches metric dimensions and weights of several tonnes (Fig. 4c), reflecting the peak of crystalline gigantism of the body — scarce nucleation and rapid growth in a residual melt enriched in fluxing components. Over this magmatic framework, kaolinisation of variable, selective and heterogeneous intensity is observed, partially to totally affecting the megacrysts in some bodies and preserving them in others, suggesting channelised percolation of hydrolytic fluids along fractures and cleavages. This zone was mined in most pegmatites of the province, since both microcline and kaolin are industrial ores (ceramics, glass), which restricts *in situ* textural characterisation to residual exposures of mining fronts.

In the Capoeira pegmatite, 100 m southwest of the main galleries, a pegmatite dyke crops out with a maximum width of 4 m and several hundred metres in length (Capoeira 2, *sensu* Soares 2004). This tabular, zoned body displays minerals denoting more extreme fractionation than the main body of the Capoeira pegmatite (Capoeira 1, *sensu* Soares, 2004, and hereafter renamed accordingly). Since its major axis was mined almost to complete exhaustion, its zonation was inferred from an unmined apophysis intruded into the enclosing metaconglomerates. This apophysis shows an atypical zonation, whose border has millimetric garnet crystals associated with a fine quartz–feldspathic matrix (Fig. 4d). As one moves towards the interior of the body, this matrix disappears abruptly, giving way to coarse equidimensional (centimetric) tourmaline crystals, associated with coarse crystals of cleavelandite, beryl and muscovite. The presence of lepidolite and spodumene in the tailings near this apophysis indicates the probable presence of this paragenesis. The spodumene found in the tailings of this pegmatite may occur as a primary mineral associated with the microcline of a hypothetical mined zone III, whereas the lepidolite may derive from the alteration of spodumene, feldspars, muscovite, tourmaline or beryl through lithium metasomatic processes, generating replacement bodies rich in lepidolite and cleavelandite.

Zone IV (core): constitutes the central portion of the pegmatite, generally filled with pink to smoky quartz, and usually has an ellipsoidal shape (Fig. 4e).

Between zones III and IV, centimetric to metric pockets composed of cleavelandite and fine muscovite occur, generally bordered by coarse muscovite, interpreted as replacement bodies (*sensu* Cameron et al. 1949). These are transgressive, subsolidus units that selectively consume the pre-existing magmatic phases by metasomatic reaction, generating albitic–micaceous assemblages comparable to greisens (Fig. 4f). The lamellar morphology of the albite (cleavelandite) and the fine grain size of the muscovite indicate growth from a fluid phase, rather than from a melt, marking the magmatic–hydrothermal transition of the system.

The metallic and gemmological mineralizations of the pegmatites — niobium-tantalates, cassiterite and beryl — occur systematically associated with these pockets, and not with the crystallisation zones, indicating that Nb, Ta, Sn and Be were partitioned into the aqueous phase exsolved from the residual melt and transported and deposited by it. In some bodies, cupriferous concretions (djurleite) are recorded at the margins of the replacement bodies, whose origin — late hydrothermal or supergene — remains to be defined.

At the contact between zones III and IV, specifically in the Mamões pegmatite, coarse green muscovite *booklets* also occur, distinct from the replacement-body muscovites by their euhedral habit, straight contacts with adjacent phases, continuous basal cleavage (001) and concordant position with the body zonation, having grown freely towards the interior; they are interpreted as primary magmatic muscovite, with no genetic relationship to the late metasomatism (Fig. 4g). This is justified because such features record growth from a medium, rather than replacement, texturally

distinguishing them from the replacement-body muscovites, which are fine-grained, with irregular contacts and a transgressive arrangement.

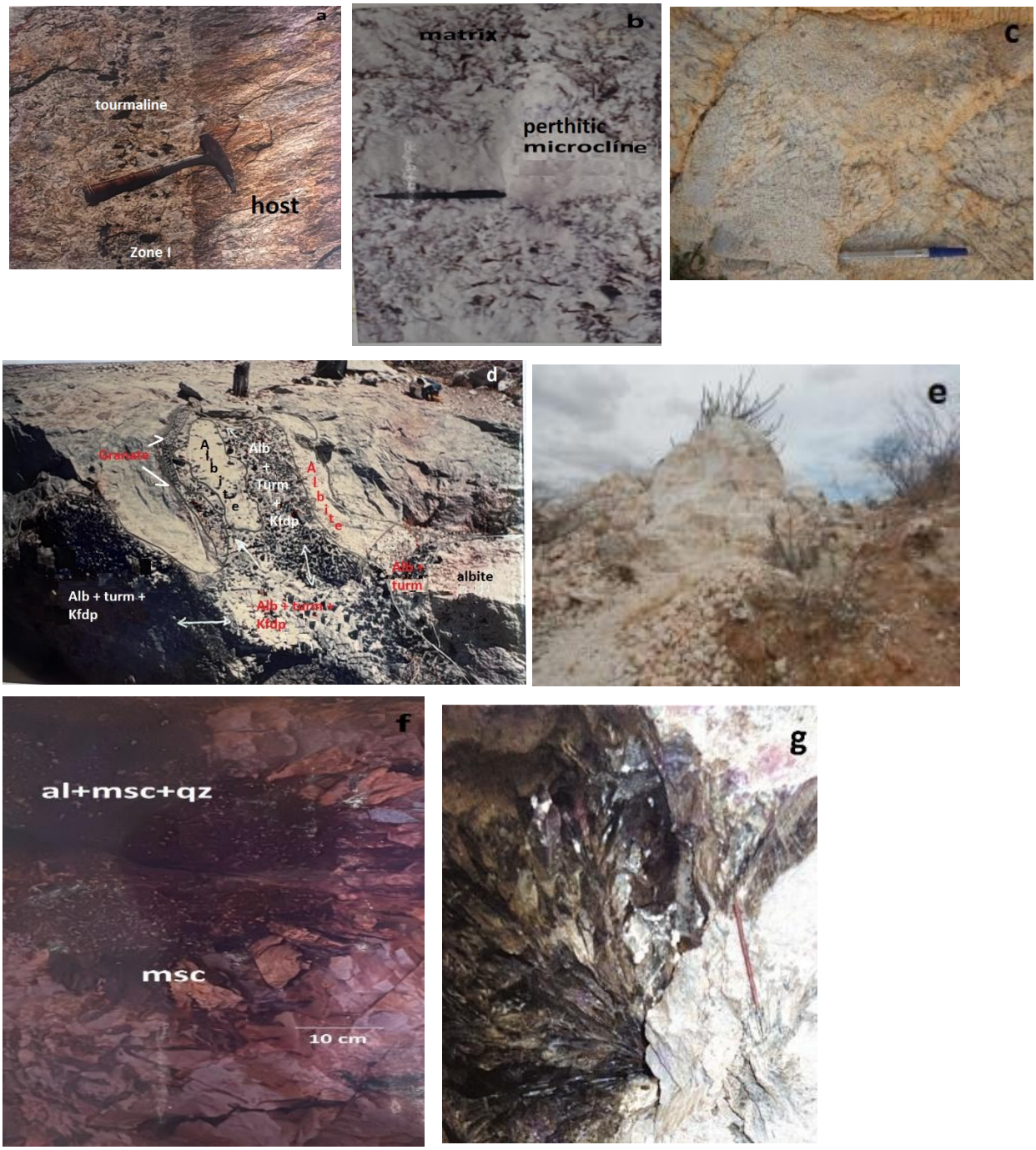

Fig. 4 General aspects of the pegmatitic facies. (a) Zone I (border) of the Capoeira 1 pegmatite, with tourmaline crystals in contact with the metaconglomerates of the Equador Formation; (b) zone II (wall) of the Mamões pegmatite, with perthitic microcline surrounded by an interstitial assemblage of quartz, plagioclase and muscovite; (c) zone III (intermediate) of the Mamões pegmatite, composed mainly of microcline; (d) apophysis in the Capoeira 1 pegmatite showing complex zonation; (e) zone IV (core) of the Mamões pegmatite, formed by pink quartz; (f) replacement bodies in the Mamões pegmatite, at the contact of zones III and IV, showing albite, muscovite and quartz bordered by coarse centimetric muscovite; and (g) coarse green muscovite booklets at the contact between zones III and IV of the Mamões pegmatite. Photographs: (a–d) the authors; (e) Sales (2020); (f, g) the authors.

Table 1 summarises the physical, mineralogical and structural characteristics of the studied pegmatites, including their coordinates, host rocks, morphology, structural orientation and dimensions.

Body	Location	Type mineralogy	Host relation	Host rock	Body shape	Orientation	Dimensions (m)
Mamões	6°55′–36°44′	Ta, Be	D	Q	L	N30E–88SE	400 × 40
Capoeira 1	6°41′–36°38′	Ta, Be, Li	D	MC	L	SE–NW	550 × 30

Table 1. Sampled heterogeneous pegmatites with their physical and mineralogical characteristics. Type mineralogy: characteristic ore minerals. Host relation: D = discordant. Host rock: Q = quartzite; MC = metaconglomerate. Body shape: L = lenticular. Orientation: strike, dip. Dimensions: length × width, in metres.

3. Materials and methods

Polished thin sections were prepared at the Universidade Federal do Rio Grande do Norte (UFRN) and examined by optical microscopy and by scanning electron microscopy (SEM) at the same institution. SEM analyses were performed on a JEOL JSM-6390 LV equipped with an Oxford Instruments ULTIM MAX 100 energy-dispersive X-ray spectrometer (EDS) and the Aztec 4.1 analytical software.

Major- and minor-element compositions were determined with a Cameca SXFive electron microprobe at the Microprobe Laboratory of the Núcleo de Litoquímica e Análises Minerais, Universidade Federal do Rio Grande do Sul (UFRGS). The analytical conditions were an accelerating voltage of 15 kV, a beam current of 20 nA and a beam diameter of 15 µm. Natural minerals and synthetic oxides were used as standards. Peak counting times were 10 s for all major and minor elements, with 5 s on each side of the background. Cs, Sr, Nb and Ta were included in the microprobe routine only for verification and remained below the detection limit of the method; the values reported here for these elements were obtained exclusively by LA-ICP-MS. Detection limits for most elements during the electron-microprobe analyses ranged between 100 and 300 ppm, and were below 100 ppm for a small subset of elements. All data were corrected using the ZAF procedure.

Lithium cannot be determined by electron microprobe; its contents were obtained directly by LA-ICP-MS and are reported as elemental Li (ppm). For comparison with literature data expressed as Li_2O, the corresponding stoichiometric conversion was applied. Fluorine was determined by electron microprobe using wavelength-dispersive spectrometry (WDS) with a multilayer crystal (2d = 61 Å). To minimise decomposition effects in the F-poor (H_2O-rich) micas, the beam was defocused to a diameter of 20–30 µm. The analytical error for the highest F concentrations was better than ±200 ppm (±0.02 wt%).

Trace-element concentrations (Sr, Rb, Cs, Ga, Zn, Li, Ta and Nb) were determined by laser-ablation inductively coupled plasma mass spectrometry (LA-ICP-MS) using a Thermo Fisher® Element2 sector-field instrument coupled to a high-performance New Wave Research® laser-ablation system with a deep-UV Nd laser (213 nm). External calibration was performed against the NIST SRM 610 reference glass, using the Al_2O_3 content previously determined by electron microprobe as the internal standard; results for the secondary reference material are given in Table S3 of the Online Resource 1. In situ analyses were carried out on exactly the same crystal regions previously analysed by electron microprobe, using the thick polished sections described above. During laser ablation, helium was used as the carrier gas and argon as the make-up gas to tune the sensitivity of the instrument. The LA-ICP-MS operating conditions were a laser fluence of 3.0 J/cm², a repetition rate of 6 Hz, a beam diameter of 30 µm and an acquisition time of 45 s, preceded by 40 s of background measurement. Detection limits for the elements determined by LA-ICP-MS are listed in Table S2 of the Online Resource 1; Sr contents (9–24 ppm) lie two to three orders of magnitude above the method detection limit and are therefore fully quantifiable. All reported trace elements were determined by LA-ICP-MS.

Sixty-four muscovite spot analyses were obtained in the two studied pegmatites, distributed across the internal zones of each body and spanning from primary magmatic domains to secondary domains of metasomatic character: in the Mamões pegmatite, zone I (n = 8), zone II (n = 7), replacement bodies (n = 11) and booklets from the contact between zones III and IV (n = 10); in the Capoeira 1 pegmatite, zone I (n = 10), zone II (n = 7) and replacement bodies (n = 11). The green muscovite booklets occur exclusively in the Mamões pegmatite and, for this reason, are analysed only within the internal context of that body. Initially, a detailed petrographic study was carried out under transmitted- and reflected-light microscopy, aiming to characterise the genetic relationships between the micas and the Nb–Ta oxides. Backscattered-electron (BSE) images were then obtained to identify inclusions that could interfere with the chemical analyses. The mean values and their respective standard deviations are presented in Table 2; the individual analyses, on which the observations of dispersion and compositional overlap are based, are given in the Online Resource 1.

	Mamões pegmatite	Capoeira 1 pegmatite

Element	ZI (n=8)	ZII (n=7)	CS (n=11)	bk (n=10)	ZI (n=10)	ZII (n=7)	CS (n=11)
Major and minor elements (wt%)							
SiO_2	45.15 (0.12)	45.04 (0.26)	44.89 (0.37)	44.1 (0.08)	45.18 (0.41)	45.06 (0.38)	44.45 (0.5)
TiO_2	0.23 (0.04)	0.24 (0.15)	0.21 (0.05)	0.13 (0.04)	0.52 (0.09)	0.53 (0.07)	0.51 (0.05)
Al_2O_3	32.96 (0.46)	34.6 (0.9)	33.36 (0.31)	34.04 (0.71)	33.11 (0.75)	33.07 (0.32)	34.24 (0.43)
Fe_2O_3T	3.2 (0.16)	2.69 (1.04)	3.3 (0.38)	3.55 (0.22)	3.25 (0.42)	3.31 (0.39)	2.92 (0.1)
MgO	0.7 (0.04)	0.84 (0.22)	1.06 (0.09)	0.59 (0.42)	0.83 (0.26)	0.89 (0.29)	0.54 (0.24)
CaO	0.05 (0.03)	0.11 (0.13)	0.03 (0.01)	0.03 (0.01)	0.03 (0.01)	0.02 (0.01)	0.11 (0.09)
Na_2O	0.69 (0.01)	0.76 (0.06)	0.65 (0.05)	0.68 (0.07)	0.71 (0.04)	0.64 (0.03)	0.65 (0.04)
MnO	0.06 (0.01)	0.06 (0.04)	0.08 (0.03)	0.15 (0.01)	0.14 (0.03)	0.11 (0.07)	0.21 (0.05)
K_2O	10.25 (0.16)	10.16 (0.1)	10.21 (0.14)	10.13 (0.31)	10.38 (0.24)	10.21 (0.09)	10.33 (0.04)
F	0.35 (0.04)	0.57 (0.15)	0.65 (0.04)	0.86 (0.05)	0.78 (0.13)	0.55 (0.23)	0.57 (0.24)
LOI	5.2 (0.21)	5.19 (0.27)	5.03 (0.13)	4.94 (0.1)	5.21 (0.07)	5.52 (0.34)	5.24 (0.25)
Total	98.84 (0.39)	100.25 (0.85)	99.47 (0.66)	99.2 (0.59)	100.12 (0.81)	99.91 (0.4)	99.78 (0.59)
Trace elements (ppm)							
Sr	14 (1)	13 (2)	14 (1)	20 (3)	18 (1)	11 (2)	20 (2)
Rb	2194 (517)	2742 (751)	3973 (594)	4892 (98)	2659 (288)	1709 (251)	3770 (1015)
Cs	50 (4)	57 (28)	93 (43)	282 (4)	35 (3)	23 (8)	146 (4)
Ga	156 (19)	151 (20)	199 (11)	244 (26)	199 (13)	153 (16)	230 (23)
Zn	152 (2)	176 (53)	187 (60)	331 (26)	264 (87)	153 (37)	331 (105)
Li	220 (12)	275 (187)	452 (214)	621 (5)	234 (43)	362 (38)	240 (6)
Ta	100 (3)	85 (29)	118 (23)	162 (28)	44 (3)	35 (6)	50 (11)
Nb	399 (64)	429 (93)	472 (49)	458 (5)	415 (84)	376 (39)	369 (44)
Geochemical ratios							
K/Rb	40.5 (8.4)	33.3 (11.1)	22 (5)	17.2 (0.7)	32.7 (2.9)	50.5 (7.2)	24.8 (8.4)
Al/Ga	1133 (155)	1231 (175)	891 (49)	746 (74)	885 (61)	1155 (128)	795 (77)
K/Cs	1707 (136)	2057 (1624)	1001 (205)	298 (9)	2496 (258)	3998 (1341)	588 (19)

Table 2. Mean chemical composition of the muscovites from the Mamões and Capoeira 1 pegmatites by zone (standard deviation in parentheses). ZI = border zone; ZII = wall zone; CS = replacement bodies; bk = booklets from the zone III–IV contact (Mamões only); LOI = loss on ignition.

4. Results and discussion

4.1. Petrographic description

The petrographic characterisation was carried out in order to discriminate, at thin-section scale, the processes responsible for the formation of each domain of the pegmatite bodies. The principle adopted here is that texture directly records the crystal growth mechanism — free growth from a medium, solid-state exsolution or replacement by reaction — whereas chemical composition records the composition of the medium, which may be shared by distinct processes when the fluid phase derives from the residual liquid itself. This distinction is central to the interpretation presented below, since muscovites of magmatic and metasomatic origin may show similar trace-element contents and yet be unequivocally distinguished by textural criteria.

Magmatic features. Quartz occurs as cuneiform to vermiform wedges lodged in a single microcline host, with simultaneous extinction under crossed nicols, recording graphic intergrowth by cotectic crystallisation. Tourmaline from zone I forms idiomorphic prisms with preserved colour zoning, and garnet forms idiomorphic millimetric crystals. In zone II, muscovite is euhedral and prismatic (2.0 × 3.5–5.0 mm in the early phases, as laths in the interstitial ones), with straight, mutual contacts. In the booklets from the contact between zones III and IV of the Mamões pegmatite, muscovite shows a book habit, continuous and intact basal cleavage (001), straight contacts and an arrangement concordant with the zonation — a criterion that distinguishes it from the replacement micas, whose cleavage is interrupted or truncated by new-generation fringes.

Exsolution features. The microcline of zones II and III displays lamellar perthite of homogeneous spacing, constant orientation and uniform distribution, resulting from subsolidus exsolution. Added to this are the grid twinning of the microcline and the polysynthetic twinning of the plagioclase, both primary. The distinction from replacement perthite — patchy, controlled by margins and fractures — is the most decisive textural criterion applicable to the feldspars (Fig. 5a).

Hydrothermal features. Although muscovite predominantly preserves magmatic crystallisation characteristics, some crystals show slightly irregular margins and microfractures that may reflect late re-equilibration processes (Fig. 5b), constituting a strong indication of the action of magmatic–hydrothermal fluids during the final stages of the system's evolution. Thus, the textural modifications observed in muscovite may reflect localised late re-equilibration by fluids derived from the residual liquid itself, rather than a distinct hydrothermal event.

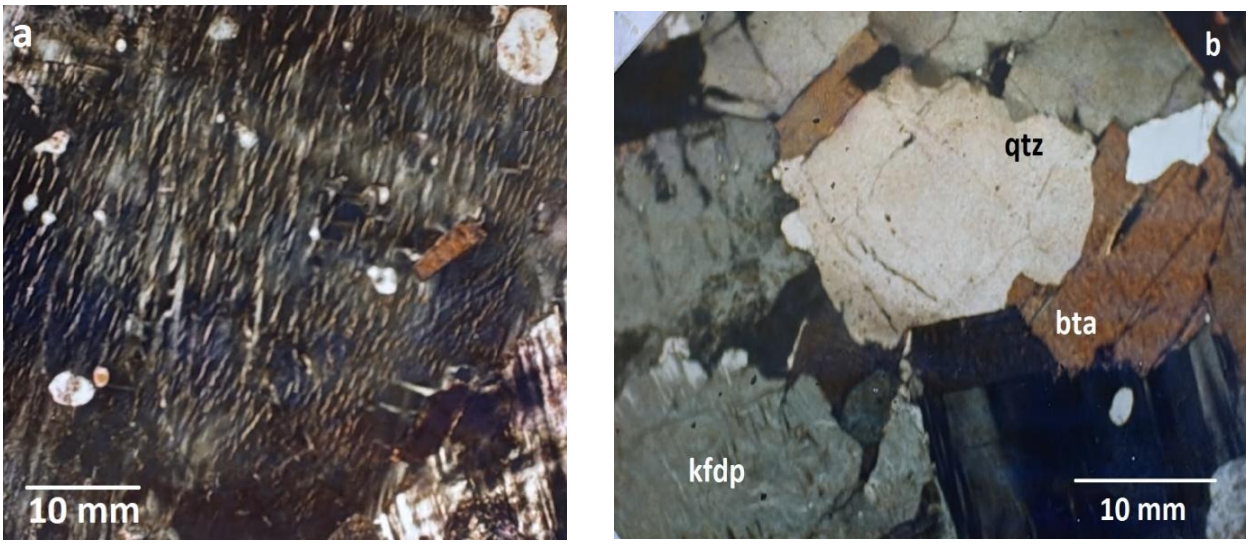

Fig. 5 Petrographic features in thin section. (a) Photomicrograph of a microcline crystal from zone II of the Mamões pegmatite, showing well-developed perthitic texture characterised by exsolved albite lamellae oriented along preferential crystallographic directions, typical of subsolidus re-equilibration in alkali feldspars of granitic pegmatites; (b) photomicrograph of a muscovite crystal from zone II of the Mamões pegmatite, showing a well-developed lamellar habit, preserved basal cleavage and slight marginal irregularities and microfractures. These features, together with the sericitisation observed in the same pegmatite body and the geochemical indicators of late evolution, suggest localised interaction with magmatic–hydrothermal fluids. Source: the authors.

Replacement features. In the replacement bodies, albite occurs as divergent, fan-shaped tabular laths advancing over the microcline from grain boundaries and microfractures (cleavelandite, sodic metasomatism). Second-generation muscovite forms fine flakes in aggregates of irregular outline and transgressive arrangement; the contrast with the euhedral booklets, observable in the same thin section, is the main textural argument for the genetic distinction between the two populations. The pre-existing phases show corroded margins, dissolution embayments and, in advanced replacement, relics immersed in the aggregate. Sericitisation, in flakes of white mica (< 50 μm) over cleavages and fractures, evidences channelised fluid percolation.
In the replacement bodies of Capoeira 1, neither lepidolite nor pseudomorphs after spodumene, feldspar or beryl are observed. The assemblage is limited to cleavelandite and fine muscovite, indicating sodic metasomatism without lithium input — consistent with the Li contents discussed below.

4.2. Analytical considerations

The analytical totals lie mostly between 98.0 and 101.0 wt%. Three analyses exceed this range (MAM-ZII-04, 101.68 %; CAP-ZI-05, 101.35 %; CAP-ZI-08, 101.32 %); in these, the high total is accompanied by simultaneously high Fe_2O_3T and Al_2O_3 contents, without the negative correlation expected between these oxides in tetrahedral- and octahedral-site substitutions, suggesting a contribution from micro-inclusions. These three analyses are retained in the dataset and in Table S1 for transparency but were excluded from the calculation of the trends discussed below; their removal does not change the mean ratios per zone beyond the respective standard deviation. A further, fourth analysis (MAM-CS-03), which simultaneously showed anomalously high Al_2O_3, low Fe_2O_3T and a total of 101.02 %, was discarded before compilation and is not listed in Table S1. The dataset discussed here therefore comprises 64 retained analyses (36 from Mamões and 28 from Capoeira 1), of which 61 enter the statistical calculations.
It should also be noted that Nb and Ta contents in muscovite must be evaluated with caution where a contribution from accessory phases rich in these elements is possible, particularly rutile, which in pegmatites may contain high Nb and Ta concentrations. In the present study the analyses were obtained *in situ*, with textural control, which minimises

this effect relative to procedures based on mineral concentrates; even so, analyses showing evidence of an inclusion contribution were discarded during data processing.
Two further observations support a largely structural incorporation of Nb and Ta in the analysed volumes. First, Nb and Ta are not positively correlated within either body (Pearson r = 0.17, p = 0.33, n = 36 at Mamões; r = −0.25, p = 0.21, n = 28 at Capoeira 1), as would be expected if a single Nb–Ta-rich accessory phase dominated the signal. Second, the highest Ta contents occur in the low-Ti booklets rather than in the more Ti-rich marginal micas, which argues against a rutile contribution to the Ta budget. The Nb and Ta contents are nonetheless treated as minimum structural estimates, and a definitive assessment would require direct analysis of the Nb–Ta oxide phases.

4.3. Major and minor elements

The stoichiometric constituents of muscovite show reduced variation between zones and between the two bodies: SiO_2 between 44.1 and 45.2 wt%, Al_2O_3 between 33.0 and 34.6 wt% and K_2O between 10.1 and 10.5 wt%. These values lie within the range expected for muscovite and do not, in themselves, constitute a distinctive characteristic of the studied bodies; their main usefulness is to attest to the compositional homogeneity of the analysed micas and, consequently, to validate the comparison of trace elements between zones.
Fe_2O_3T contents vary between 2.7 and 3.6 wt% and warrant specific mention, since Fe^{3+} significantly occupies the tetrahedral sites of the muscovite structure, competing with Al and influencing the crystallochemical parameters used in the comparison between mica generations. It is also observed that Fe_2O_3T, Al_2O_3 and SiO_2 maintain among themselves the negative correlation expected in substitutions at these sites.
Against this relatively invariant background, two behaviours are worth noting. The first is that of TiO_2, which systematically discriminates the two pegmatites: the Capoeira 1 contents (0.51–0.53 %) are about twice those of Mamões (0.21–0.24 %) in all homologous zones, constituting an inherited characteristic, probably related to the composition of the parental liquid or to interaction with the host rock. Within each body, TiO_2 remains constant from the border to the replacement bodies, decreasing only in the Mamões booklets (0.128 ± 0.038 %), which is compatible with the more evolved character of this population. The second is that of fluorine, the only major constituent to show a pronounced monotonic trend, and only in the Mamões pegmatite, in which it increases about two and a half times from the marginal zones to the booklets (0.349 ± 0.042 → 0.856 ± 0.046 wt%). Considering the analytical error of the F determination (±0.02 wt%), this variation corresponds to more than ten times the dispersion of the populations and constitutes an unequivocal trend. In Capoeira 1 no equivalent trend is observed: the differences between zones (0.775 to 0.553 %) lie at about 1 σ of the internal dispersion, which is high in this body (coefficients of variation of 17 to 43 %, against 5 to 12 % at Mamões). MnO follows the fractionation at Mamões, increasing from 0.06 % in the marginal zones to 0.15 % in the booklets.
The restriction of the fluorine increase to Mamões is spatially coincident with its stronger Ta enrichment and falling Nb/Ta (Section 4.5). Because fluorine complexing is known to enhance the solubility and mobility of high-field-strength elements in evolved granitic melts (Sami et al. 2025; Zheng et al. 2025), the coupled rise of F and Ta at Mamões is consistent with a residual liquid that became progressively enriched in fluxing and incompatible components; we describe this as an empirical association and do not infer a causal control from the present data alone.
Structural formulae were calculated on the basis of 22 oxygen equivalents, with all iron as Fe^{2+} and rubidium assigned to the interlayer (X) site (individual analyses in Table S1; mean values by zone in Table S5). The analysed micas are dioctahedral, with Si between 6.01 and 6.27 apfu, tetrahedral Al (Al^{IV}) of 1.73–1.99 apfu and octahedral Al (Al^{VI}) of 3.42–3.78 apfu, confirming a muscovite composition throughout. The interlayer site is occupied mainly by K (1.71–1.89 apfu) with subordinate Na (0.15–0.23 apfu) and minor Rb (0.014–0.049 apfu), and shows a small vacancy (up to 0.08 apfu) that increases slightly in the most fractionated populations. Octahedral Fe (0.12–0.40 apfu) and Mg (0.02–0.25 apfu) substitute for Al^{VI} through the Tschermak-type exchange $(Fe,Mg)^{2+} + Si^{4+} \rightleftarrows Al^{VI} + Al^{IV}$, consistent with the negative Si–Al correlation noted above, while the incorporation of Li and the progressive substitution of F for OH (up to 0.43 apfu F at Mamões) reflect the phengitic and fluorine-rich character acquired by the most evolved populations. These crystal-chemical trends parallel the trace-element evolution and reinforce the link between muscovite composition and the degree of magmatic differentiation.

4.4. Trace elements and fractionation ratios

The K/Rb, K/Cs and Al/Ga ratios, traditionally used as fractionation indicators in granitic pegmatites (Beus 1966; Gordyienko 1971; Trueman and Černý 1982), record a progressive evolution from the marginal to the internal zones in both bodies (Fig. 6a). In the Mamões pegmatite, the K/Rb ratio decreases from 40.5 ± 8.4 in the border zone to 22.0 ± 4.9 in the replacement bodies and 17.2 ± 0.7 in the booklets, accompanied by a decrease in Al/Ga (1133 → 746) and increases in Rb (2194 → 4892 ppm), Cs (50 → 282 ppm) and Ga (156 → 244 ppm). The Capoeira 1 pegmatite

describes an equivalent, though shorter, trajectory, from K/Rb 32.7 ± 2.9 in zone I to 24.7 ± 8.4 in the replacement bodies, with Al/Ga from 885 to 795. In both bodies, zone II departs slightly from the monotonic trend, showing Al/Ga ratios higher than those of zone I, which is attributed to the marked textural and granulometric heterogeneity of this unit.

The two pegmatites are not equivalent in degree of evolution, and the most robust discriminant is tantalum. The Mamões muscovites systematically contain 45–197 ppm Ta, whereas those of Capoeira 1 do not exceed 26–74 ppm — a two- to threefold difference preserved in all homologous zones. Conversely, the replacement bodies of Capoeira 1 concentrate more caesium (146 ± 4 ppm against 93 ± 43 ppm at Mamões), which is reflected in the Ta/Cs ratios (0.34 and 1.36, respectively). The two bodies therefore record distinct fractionation trajectories: Mamões evolves preferentially in high-field-strength elements (Ta, Nb), whereas Capoeira 1 advances comparably in rare alkalis, without matching the Ta enrichment. This divergence is internal to the muscovites and describes the behaviour of the magmatic system; its translation into terms of mineral potential requires data of a different nature, discussed below.

The behaviour of lithium distinguishes the two bodies as to the nature of the late metasomatism. In the Mamões pegmatite, the Li contents in the replacement-body muscovites (452 ± 214 ppm) are twice those recorded in the border zone (220 ± 12 ppm), indicating effective input of this element by the fluid phase. In the Capoeira 1 pegmatite, by contrast, the contents remain practically unchanged between the border zone (234 ± 43 ppm) and the replacement bodies (240 ± 6 ppm), despite the marked increase in Cs (35 to 146 ppm) over the same interval. The replacement bodies of Capoeira 1 therefore record sodic metasomatism — expressed by the cleavelandite described in the field — without associated lithium metasomatism (Fig. 6b). This result is consistent with the observations of Pereira (2000), according to which the lepidolite- and cleavelandite-rich replacement bodies occur in the Capoeira 2 pegmatite — a more fractionated satellite body situated about 100 m southwest of the main galleries — and not in the Capoeira 1 studied here. Muscovite chemistry thus provides independent confirmation of the difference in degree of fractionation between the two bodies of the Capoeira pegmatite field.

4.5. Nb/Ta and Li/Rb ratios: fractionation degree and the primary character of the muscovites

Because Nb and Ta behave as incompatible high-field-strength elements that are progressively fractionated during pegmatite crystallisation, the Nb/Ta ratio of muscovite is widely used both as a fractionation index and as a discriminant between magmatic and hydrothermal micas (Jolliff et al. 1992; Ballouard et al. 2016; Li et al. 2021). In the studied bodies, Nb/Ta separates the two pegmatites clearly. Capoeira 1 shows generally higher values (4.2–14.6; zone means 7.8–10.9), whereas Mamões shows lower ratios (2.3–7.7; zone means 4.0–5.5), overlapping the Nb/Ta = 5 reference only in its wall zone. This contrast is coherent with the divergent trajectories inferred from K/Rb and Ta/Ga (Section 4.4): Mamões fractionates preferentially towards Ta (lowering Nb/Ta), while Capoeira 1 preserves higher Nb/Ta as it advances in rare alkalis (Fig. 7a).

Within each body, Nb/Ta and K/Rb decrease together from the border and wall zones towards the replacement bodies, defining a positive covariation ($r = 0.62$ at Capoeira 1; $r = 0.31$ at Mamões; Fig. 7b). This coupled decrease is the trend expected for progressive magmatic fractionation and matches that described for primary muscovite in other rare-element granite–pegmatite systems, in which Rb, Cs and Nb increase while K/Rb and Nb/Ta fall (Li et al. 2021; Zheng et al. 2025). It thus provides an additional, chemically independent argument that the analysed grains — including the euhedral booklets of Mamões — record magmatic crystallisation rather than a later replacement event.

The magmatic character is reinforced by the Li/Rb–Nb/Ta relationship (Fig. 7c). Magmatic muscovite is commonly characterised by high Nb/Ta (typically > 5) combined with low to moderate Li/Rb, whereas hydrothermal micas from greisen tend to show both ratios depressed (Monnier et al. 2022; Li et al. 2021); this contrast is used here as a supporting criterion, not as a stand-alone discriminant. All but one of the Capoeira 1 analyses, and the Mamões wall-zone analyses, fall within the magmatic field (Nb/Ta > 5), with Li/Rb below 0.30 throughout; no analysis plots in the low-Nb/Ta, low-Li/Rb domain associated with pervasive greisenisation. It should be stressed, however, that a substantial part of the Mamões dataset has Nb/Ta < 5 (2.7–7.7), so Nb/Ta alone does not resolve the magmatic versus hydrothermal question. Evaluated together with the euhedral habit and continuous basal cleavage of the grains (Section 4.3) and with the Li/Rb systematics, the data are consistent with a dominantly magmatic signature rather than with pervasive fluid overprinting.

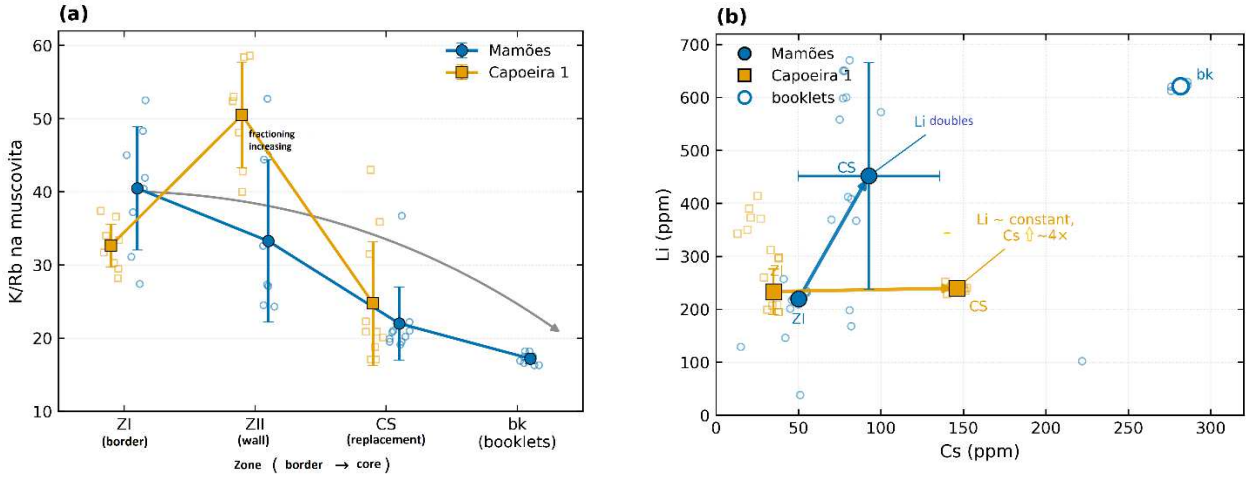

Fig. 6 Compositional evolution of the muscovites by zone. (a) K/Rb ratio from margin to core in the Mamões and Capoeira 1 pegmatites; smaller symbols are individual analyses and larger ones are the zone means (bars = ±1 standard deviation). (b) Cs vs Li diagram (ppm); arrows link the border-zone (ZI) mean to that of the replacement bodies (CS) of each body. At Mamões, Li and Cs increase together from margin to core; at Capoeira 1, Cs increases about fourfold while Li remains practically constant, evidencing sodic metasomatism without lithium input. bk = booklets from the zone III–IV contact, present only at Mamões. Source: the authors.

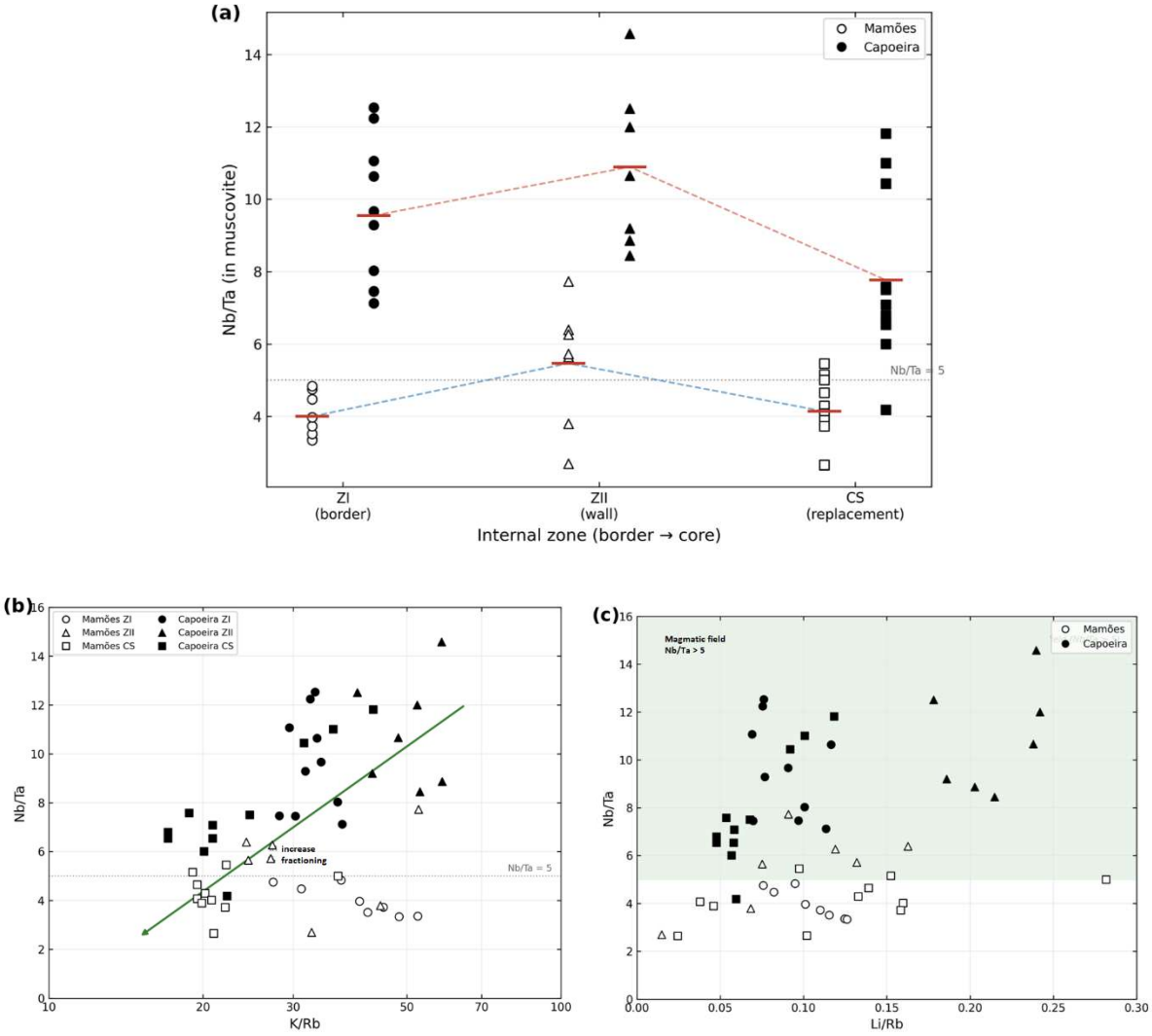

Fig. 7 Nb/Ta and Li/Rb systematics of the muscovites. (a) Nb/Ta by internal zone (border → core); red dashes are zone means, dashed lines link the means of each body. (b) Nb/Ta vs K/Rb; the two ratios decrease together towards the more fractionated compositions (green arrow). (c) Li/Rb vs Nb/Ta; the shaded band marks the magmatic field (Nb/Ta > 5). Open symbols: Mamões; filled symbols: Capoeira 1. Circles = zone I; triangles = zone II; squares = replacement bodies (CS). Source: the authors.

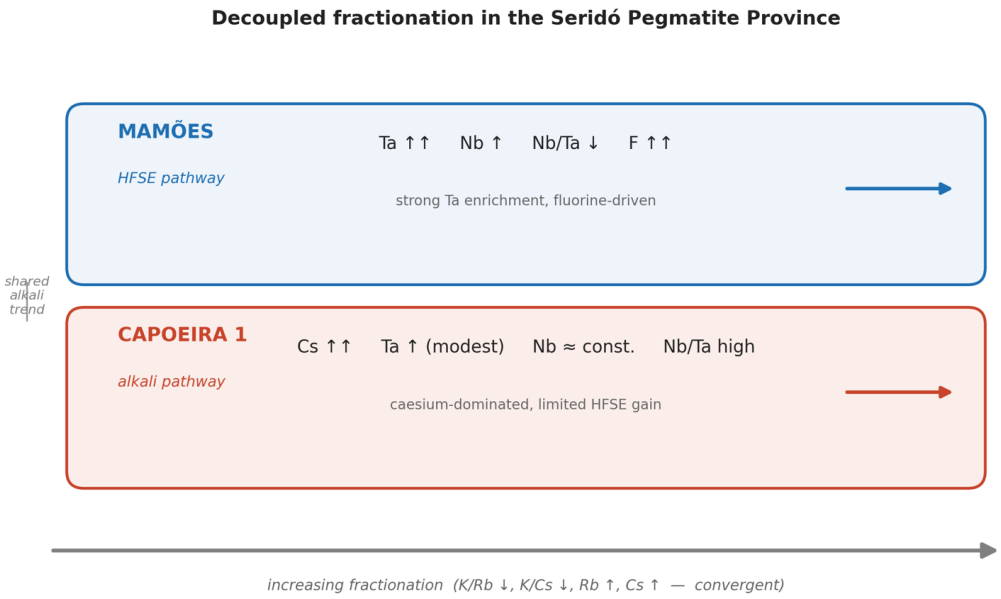

Fig. 8 Conceptual summary of the decoupled fractionation recorded by muscovite in the two pegmatites. Both bodies share a convergent alkali trend (falling K/Rb and K/Cs; rising Rb and Cs), but their high-field-strength-element evolution diverges: Mamões follows a Ta- and F-enriched pathway with decreasing Nb/Ta, whereas Capoeira 1 follows a caesium-dominated pathway with only modest Ta gain and comparatively high Nb/Ta. Source: the authors.

4.6. Decoupled fractionation of high-field-strength elements and rare alkalis

Taken together, the ratios examined above describe two processes that operate to different extents in the two bodies. The rare alkalis define a convergent trend: Rb and Cs increase together from margin to core in both pegmatites (Rb–Cs Pearson $r = 0.79$, $p < 10^{-8}$, $n = 36$ at Mamões; $r = 0.73$, $p < 10^{-5}$, $n = 28$ at Capoeira 1), and K/Rb and K/Cs decrease accordingly. The high-field-strength elements, in contrast, diverge. At Mamões, Ta rises strongly (45 to 197 ppm), Nb increases more modestly and Nb/Ta consequently falls (zone means from 5.5 in the wall zone to 2.9 in the booklets), while fluorine climbs from about 0.16 to 0.40 apfu. At Capoeira 1, Ta gains only modestly, Nb remains nearly constant, Nb/Ta stays comparatively high (means 7.8–10.9) and fluorine shows no comparable rise. Notably, Nb and Ta are uncorrelated within each body ($r = 0.17$, $p = 0.33$ at Mamões; $r = -0.25$, $p = 0.21$ at Capoeira 1), so their ratio varies independently of the absolute concentrations.

The two pegmatites therefore record convergent alkali fractionation but divergent HFSE evolution. This contrast is summarised in Fig. 8. This decoupling shows that muscovite fractionation in the Seridó Pegmatite Province is not a single-dimensional process that can be captured by K/Rb alone: bodies that share a common alkali trend can follow distinct Ta–Nb pathways. A comparable decoupling of Ta from Nb, driven by the efficiency of muscovite in fractionating the two elements and modulated by fluorine- and water-rich residual melts, has been documented in other LCT systems (Kaeter et al. 2018; Ballouard et al. 2016; Sami et al. 2025). At Mamões the coupled rise of F, Ta and Rb–Cs with falling K/Rb and Nb/Ta is consistent with progressive concentration of incompatible and fluxing components in the residual melt; the muted Ta and F evolution of Capoeira 1 indicates that its exposed zones did not reach the same degree of HFSE enrichment. We stress that these covariations are described here as empirical trends and are not used to infer a specific causal mechanism, which would require whole-rock data and the study of Nb–Ta oxide phases (Section 4.8).

4.7. Comparison with pegmatites from other provinces

In comparison with granitic pegmatites from other provinces (Fig. 9a), the muscovites of the studied bodies plot in the high-Ta/Cs portion of the diagram, above the Ta/Cs = 1:3 line, with ratios ranging from 0.34 to 2.13. The dataset overlaps the Noumas field and zones I and II described by Da Silva (1993) in the Borborema Pegmatite Province, and plots away from the Tanco and Hagendorf fields — whose Cs contents exceed 10^3 ppm, against a maximum of 286

ppm in the present study — lying above Osis Lake and Pullersreuth, bodies of lower fractionation degree. This positioning characterises intermediate- to advanced-fractionation pegmatites of the LCT family, with asymmetric evolution: marked in high-field-strength elements and restrained in rare alkalis, without reaching the degree of the petalite–lepidolite-class bodies.

In the Ta vs Ga diagram (Fig. 9b), the distinction between the two pegmatites is clear: 35 of the 36 Mamões pegmatite analyses lie above the threshold of Gordyienko (1971), against only 2 of the 28 Capoeira 1 analyses, both in replacement bodies; all samples exceed the threshold of Beus (1966). It is necessary, however, to delimit the scope of this observation. Muscovite chemistry constitutes a preliminary prospecting vector, useful for guiding the search for comparatively more fractionated bodies or internal zones, but it does not, in itself, provide a basis for qualifying individual bodies as economically promising or barren. The thresholds of Beus (1966) and Gordyienko (1971) were established as empirical screening criteria, and their exceedance indicates compositional affinity with mineralized systems, not the presence of economically significant mineralization. In the present study, no data were obtained on the abundance and distribution of columbite-group minerals, representative whole-rock contents or the spatial persistence of the observed enrichment. It is therefore concluded that the Mamões pegmatite deserves further mineralogical and geochemical investigation of its Ta–Nb content, without Capoeira 1 being characterisable as barren on the basis of the present dataset. A defensible assessment of the mineral potential would require the identification and direct analysis of rare-element-bearing phases, representative whole-rock or channel sampling, documentation of the distribution of the enriched zones and demonstration that the signal recorded in the muscovites is accompanied by the corresponding mineral phases.

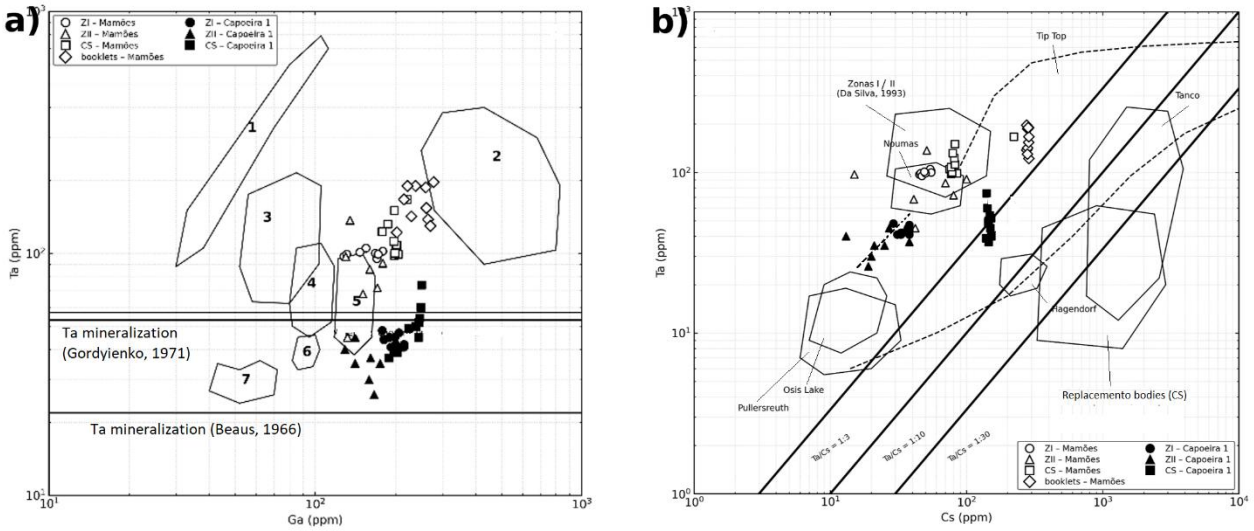

Fig. 9 (a) Ta vs Cs (ppm) diagram, with Ta/Cs ratio lines after Beus (1966) and the empirical Ta-mineralization thresholds of Beus (1966) and Gordyienko (1971); (b) Ta vs Ga (ppm) diagram, with comparison fields redrawn from Da Silva (1993) and Gaupp et al. (1984): 1 = replacement bodies (Da Silva 1993); 2 = Tanco (Gaupp et al. 1984); 3 = zones I and II and peraluminous granites (Da Silva 1993); 4 = Harding (Gaupp et al. 1984); 5 = Tip Top (Gaupp et al. 1984); 6 = Etta (Gaupp et al. 1984); and 7 = homogeneous pegmatites (Da Silva 1993), for the muscovites of the Mamões and Capoeira 1 pegmatites, together with the compositional fields of pegmatites from other provinces. Each symbol corresponds to an individual analysis.

In the K/Rb vs Ga diagram (Fig. 10a), the samples define a linear fractionation trend, with the zone I and II muscovites occupying the upper portion and those of the replacement bodies and booklets the lower portion, of low K/Rb ratio and high Ga contents. The analysed muscovites show Ga contents higher than those recorded by Da Silva (1993) for the equivalent zones of the same province, and plot in a position distinct from that of the Pegmatoid Granite (Pereira 2000), which is compatible with a more advanced differentiation stage relative to the granitic source.

Fig. 10b shows the variation and mean of the Ta contents in micas from various pegmatite provinces worldwide. Considering that the Tanco and Witkopie (Namibia) pegmatites are regarded as strongly Ta-mineralized (Möller and Morteani 1987), the Capoeira 1 pegmatite aligns chemically with bodies of low Ta enrichment (e.g., Tip Top, Buckclaim, among others), whereas the Mamões pegmatite shows significant rare-element contents (Ta up to 197 ppm; Cs up to 286 ppm), similar to Noumas, Silverleaf and the secondary micas of Tanco.

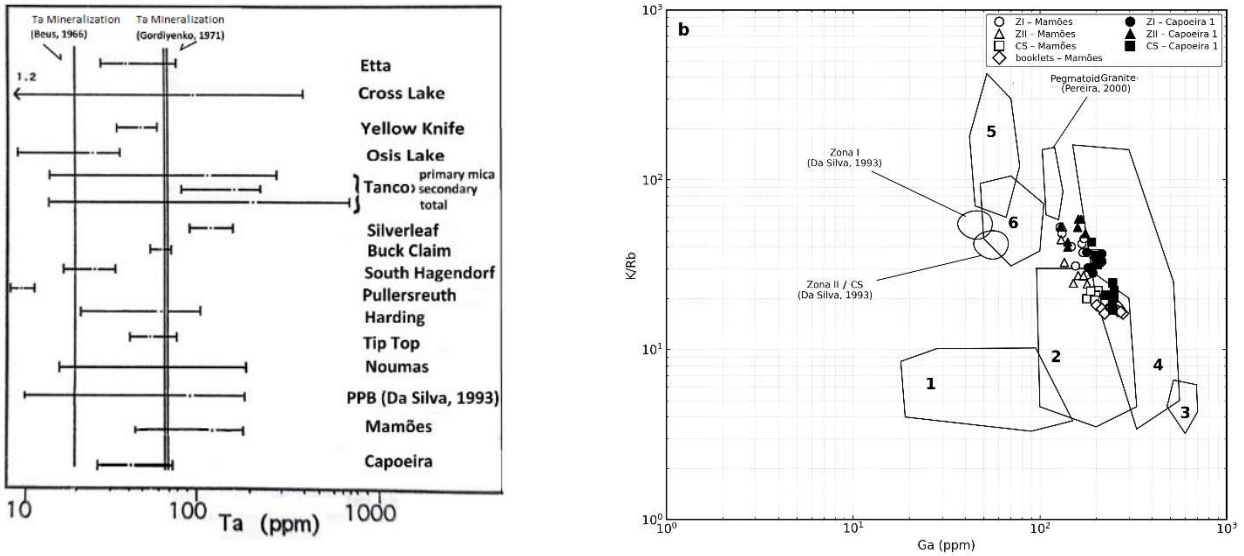

Fig. 10 (a) K/Rb vs Ga (ppm) diagram. The numbered fields correspond to reference pegmatites; also indicated are the field of the zones described by Pereira (2000) and Da Silva (1993) in the Borborema Pegmatite Province and the granite–pegmatite system in Mozambique and at Tanco (Černý and Burt 1984): 1 = anorogenic granite of Mozambique (Černý and Burt 1984); 2 = spodumene-bearing lepidolite-type pegmatite (Černý and Burt 1984); 3 = Tanco complex type (Černý and Burt 1984); 4 = lepidolite type (Černý and Burt 1984); 5 = muscovite class (Černý and Burt 1984); 6 = beryl–columbite type (Černý and Burt 1984). (b) Mean Ta contents in muscovite from various world provinces compared with the muscovites of the Seridó Geopark pegmatites.

4.8. Muscovite from the zone III–IV contact (Mamões pegmatite)

The green muscovite booklets occur exclusively in the Mamões pegmatite and constitute the most fractionated population of that body (K/Rb 17.2; Al/Ga 746; Cs 282 ppm; Ta 162 ppm), plotting at the evolved end of all diagrams. In these indices, they overlap the replacement-body muscovites of the same pegmatite. Such overlap is the expected behaviour — and not an inconsistency — when the fluid phase responsible for generating the replacement bodies derives from the pegmatitic residual liquid itself, from which it inherits the trace-element signature (London 2008). In this context, the absolute contents of Rb, Cs and Ga and the K/Rb, K/Cs and Al/Ga ratios lose discriminating power between magmatic crystallisation and hydrothermal re-equilibration, since both processes share the same geochemical source.

The genetic distinction between the two populations rests on two sets of evidence independent of the absolute contents. The first is textural, already detailed in the petrography: euhedral habit, intact basal cleavage (001) and straight contacts in the booklets, against fine habit and transgressive arrangement in the replacement micas.

The second set of evidence is the structure of the compositional variation (Fig. 11a). The booklet muscovites show minimal internal dispersion — coefficients of variation of 2.0 % for Rb, 1.4 % for Cs, 0.8 % for Li and 4.0 % for K/Rb (n = 10) — whereas those of the replacement bodies of the same pegmatite show an order-of-magnitude higher dispersion (15.0 %, 46.4 %, 47.3 % and 22.6 %, respectively, n = 11; Fig. 11b). This homogeneity is consistent with crystallisation from a single, compositionally homogeneous residual liquid, whereas the high variance of the replacement-body muscovites reflects fluid–rock reaction in an open system, in which the product depends on the local percolation conditions and the mineral assemblage consumed. The convergence between the textural criteria and the structure of the chemical variation indicates a primary magmatic origin for the booklets, crystallised at the core margin from the terminal residual liquid, and not as a product of the metasomatism that generated the replacement bodies.

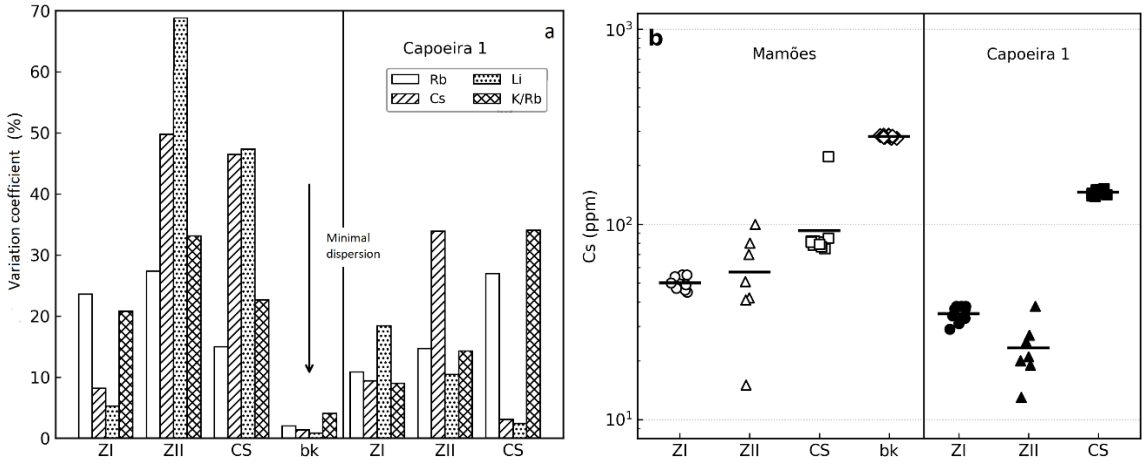

Fig. 11 Structure of the compositional variation of the muscovites by zone. (a) Coefficient of variation of Rb, Cs, Li and K/Rb; (b) distribution of the individual Cs analyses, on a logarithmic scale, with the means indicated by horizontal dashes. Symbols as in Fig. 10. bk = booklets (Mamões only).

It should be noted that the available data document a transition between a magmatic stage and a stage of re-equilibration by fluids derived from the system itself, without it being possible to demonstrate, with the present dataset, the existence of multiple distinct magmatic–hydrothermal episodes. The observed evolution is compatible with a continuous process, in which the fluid phase is exsolved from the residual liquid at the end of crystallisation.

5. Conclusions

The mineralogical and geochemical study of muscovite from the Mamões and Capoeira 1 pegmatites, based on 64 spot analyses across their internal zones, supports the following conclusions.

(1) In both bodies the K/Rb, K/Cs and Al/Ga ratios record a progressive compositional evolution from the marginal to the internal zones, with the replacement bodies and, at Mamões, the booklets from the zone III–IV contact occupying the most fractionated end of the trends.

(2) The two pegmatites follow distinct fractionation trajectories. Alkali enrichment is convergent — Rb and Cs increase together in both — but the high-field-strength elements diverge: Ta and Nb evolution becomes decoupled from the Rb–Cs trend between the two bodies.

(3) Mamões evolves preferentially in high-field-strength elements, with strong Ta enrichment (45–197 ppm), falling Nb/Ta and a marked rise in fluorine.

(4) Capoeira 1 shows a more pronounced caesium evolution, with comparatively modest Ta gain, near-constant Nb and relatively high Nb/Ta.

(5) The euhedral booklets of Mamões, distinguished from replacement-body micas by their habit and by an order-of-magnitude lower compositional dispersion, are interpreted — together with petrographic relationships and Li/Rb systematics — as primary magmatic muscovite, whereas the replacement-body micas formed by fluid–rock reaction.

(6) Muscovite chemistry indicates Ta–Nb fertility, most clearly at Mamões, but does not demonstrate economic mineralization; it constitutes a preliminary prospecting vector rather than a resource assessment.

(7) A definitive evaluation of the Ta–Nb potential will require the identification and direct analysis of the Nb–Ta oxide phases (columbite-group minerals, rutile), representative whole-rock sampling and documentation of the spatial distribution of the enrichment.

Beyond its petrogenetic interest, the Capoeira pegmatite field — which includes the type locality of the cuprian elbaite known as Paraíba tourmaline — also holds geoheritage value that could be formally assessed within the Seridó UNESCO Global Geopark.

Statements and Declarations

Funding

This research did not receive any specific grant from funding agencies in the public, commercial, or not-for-profit sectors.

Author contributions

Luciano Schaefer Pereira: Conceptualization, Methodology, Investigation, Formal analysis, Writing – original draft, Visualization. Marcos Antônio Leite do Nascimento: Conceptualization, Supervision, Validation, Writing – review & editing. [CRediT roles to be confirmed by the authors.]

Competing interests

The authors declare that they have no known competing financial interests or personal relationships that could have appeared to influence the work reported in this paper.

Data availability

The muscovite analytical dataset supporting the findings of this study is openly available in Mendeley Data at https://doi.org/10.17632/gzgcwpj9wf.1. Summary values are also provided within the article and its Online Resource 1.

References

Ballouard C, Poujol M, Boulvais P, Branquet Y, Tartèse R, Vigneresse J-L (2016) Nb–Ta fractionation in peraluminous granites: a marker of the magmatic–hydrothermal transition. Geology 44:231–234. https://doi.org/10.1130/G37475.1

Almeida FFM, Hasui Y, Brito Neves BB, Fuck RA (1981) Brazilian structural provinces: an introduction. Earth-Sci. Rev. 17:1–29. https://doi.org/10.1016/0012-8252(81)90003-9

Beurlen H, Thomas R, da Silva MRR, Müller A, Rhede D, Soares DR (2014) Perspectives for Li- and Ta-mineralization in the Borborema Pegmatite Province, NE Brazil: a review. J. South Am. Earth Sci. 56:110–127.

Beus AA (1966) Geochemistry of Beryllium and Genetic Types of Beryllium Deposits. W.H. Freeman, San Francisco, 401 pp.

Bezerra MS, Carvalho VGD, Nesi JR (1994) Caracterização e mercado de minerais de pegmatitos da Borborema. CPRM, Recife, 50 pp.

Cameron EN, Jahns RH, McNair AH, Page LR (1949) Internal Structure of Granitic Pegmatites. Economic Geology Monograph 2. Economic Geology Publishing Co., Urbana, 115 pp.

Černý P (1982) Anatomy and classification of granitic pegmatites. In: Černý, P. (Ed.), Granitic Pegmatites in Science and Industry. Mineralogical Association of Canada, Short Course Handbook 8, pp. 1–39.

Černý P, Burt DM (1984) Paragenesis, crystallochemical characteristics and geochemical evolution of micas in granitic pegmatites. In: Bailey, S.W. (Ed.), Micas. Reviews in Mineralogy 13. Mineralogical Society of America, Washington, DC, pp. 257–297.

Černý P, Meintzer RE, Anderson AJ (1985) Extreme fractionation in rare-element granitic pegmatites: selected examples of data and mechanisms. Can. Mineral. 23:381–421.

Costa SSS, Nascimento MAL, Silva MLN (2024a) Correlating geodiversity and mining in the Seridó UNESCO Global Geopark: spatial and impact analysis in Brazilian northeast. Resour. Policy 95, 105196.

Costa SSS, Nascimento MAL, Silva MLN (2024b) Geological and mining heritages in the Seridó UNESCO Global Geopark: Ediacaran to Cambrian mineral deposits revealed by historical mines in Northeast Brazil. Int. J. Geoheritage Parks 12:311–332.

[dataset] [Author(s)] (2026) Muscovite major-, minor- and trace-element chemistry of the Mamões and Capoeira zoned pegmatites, Seridó Pegmatite Province (NE Brazil). Mendeley Data, v1. https://doi.org/10.17632/gzgcwpj9wf.1

Da Silva MRR (1993) Petrographical and Geochemical Investigations of Pegmatites in the Borborema Pegmatitic Province of Northeastern Brazil (Ph.D. thesis). Ludwig-Maximilians-Universität München, Munich, Germany.

Da Silva MRR, Höll R, Beurlen H (1995) Borborema Pegmatitic Province: geological and geochemical characteristics. J. South Am. Earth Sci. 8:355–364.

Monnier L, Salvi S, Melleton J, Bailly L, Beziat D, de Parseval P, Gouy S, Lach P (2022) Mica trace-element signatures: highlighting superimposed events during the emplacement of the Beauvoir rare-metal granite (France). Chem. Geol. 600, 120866. https://doi.org/10.1016/j.chemgeo.2022.120866

Gaupp R, Möller P, Morteani G (1984) Tantal-Pegmatite: Geologische, petrologische und geochemische Untersuchungen. Monograph Series on Mineral Deposits 23. Gebrüder Borntraeger, Berlin/Stuttgart, 124 pp.

Gordyienko VV (1971) Concentrations of Li, Rb and Cs in potash feldspar and muscovite as criteria for assessing the rare-metal mineralization in granite pegmatites. Int. Geol. Rev. 13:134–142. https://doi.org/10.1080/00206817109475411

Johnston Jr. WD (1945) Os pegmatitos beril-tantalíferos da Paraíba e Rio Grande do Norte, no nordeste do Brasil. Divisão de Fomento da Produção Mineral, Rio de Janeiro.

Jolliff BL, Papike JJ, Shearer CK (1992) Petrogenetic relationships between pegmatite and granite based on geochemistry of muscovite in pegmatite wall zones, Black Hills, South Dakota, USA. Geochim. Cosmochim. Acta 56:1915–1939. https://doi.org/10.1016/0016-7037(92)90320-I

Kaeter D, Barros R, Menuge JF, Chew DM (2018) The magmatic–hydrothermal transition in rare-element pegmatites from southeast Ireland: LA-ICP-MS chemical mapping of muscovite and columbite–tantalite. Geochim. Cosmochim. Acta 240:98–130. https://doi.org/10.1016/j.gca.2018.08.024

Li P, Li J, Chou I-M, Wang D, Xiong X (2021) Compositional evolution of the muscovite of Renli pegmatite-type rare-metal deposit, northeast Hunan, China: implications for its petrogenesis and mineralization potential. Ore Geol. Rev. 138, 104380. https://doi.org/10.1016/j.oregeorev.2021.104380

London D (2008) Pegmatites. Canadian Mineralogist Special Publication 10. Mineralogical Association of Canada, Québec, 347 pp.

Miller CF, Stoddard EF, Bradfish LJ, Dollase WA (1981) Composition of plutonic muscovite: genetic implications. Can. Mineral. 19:25–34.

Möller P, Morteani G (1987) Geochemical exploration guide for tantalum pegmatites. Econ. Geol. 82:1888–1897.

Moraes JFS (1999) Gemas do Estado do Rio Grande do Norte. CPRM/Governo do RN, Recife, 72 pp.

Nascimento MAL (2018) Geoparque Seridó (RN) e suas feições geomorfológicas. Rev. Geogr. (Recife) 35:394–411. https://doi.org/10.51359/2238-6211.2018.238238

Pereira LS (2000) Geoquímica de micas e feldspatos dos pegmatitos e granitos pegmatóides da região de Parelhas/RN (M.Sc. dissertation). Universidade Federal do Rio Grande do Norte, Natal, 154 pp.

Rieder M, Cavazzini G, D'yakonov YS, Frank-Kamenetskii VA, Gottardi G, Guggenheim S, Koval PV, Müller G, Neiva AMR, Radoslovich EW, Robert J-L, Sassi FP, Takeda H, Weiss Z, Wones DR (1998) Nomenclature of the micas. Can. Mineral. 36:905–912.

Rinaldi R, Černý P, Ferguson RB (1972) The Tanco pegmatite at Bernic Lake, Manitoba. VI. Lithium-rubidium-cesium micas. Can. Mineral. 11:690–707.

Rolff PAMA (1945) Geologia da província tântalo-glucinífera da Borborema. Bol. Div. Fom. Prod. Min. 73:33–72.

Sales MCC (2020) Considerações sobre os granitos pegmatíticos da Província Pegmatítica do Seridó: mapeamento geológico e geoquímica (Undergraduate thesis). Universidade Federal do Rio Grande do Norte, Natal, 102 pp.

Sami M, Azer MK, Abdelfadil KM (2025) Crystal-chemical evolution of muscovite and Nb–Ta–Y–REE-bearing minerals in the Wadi Al-Baroud granite–pegmatite system, Eastern Desert, Egypt. Minerals 15, 1206. https://doi.org/10.3390/min15111206

Santos EJ, Souza Neto JA, Silva MRR, Beurlen H, Cavalcanti JAD, Silva MG, Costa AF, Santos LCML, Santos RB (2014) Metalogênese das porções norte e central da Província Borborema. In: Silva, M.G., Neto, M.B.R., Jost, H., Kuyumjian, R.M. (Eds.), Metalogênese das Províncias Tectônicas Brasileiras. CPRM, Brasília, pp. 343–388.

Scorza EP (1944) Província pegmatítica da Borborema (nordeste do Brasil). DNPM, Divisão de Geologia e Mineralogia, Rio de Janeiro.

Soares DR (2004) Contribuição à petrologia de pegmatitos mineralizados em elementos raros e elbaítas gemológicas da Província Pegmatítica da Borborema, Nordeste do Brasil (Ph.D. thesis). Universidade Federal de Pernambuco, Recife, 271 pp.

Trueman DL, Černý P (1982) Exploration for rare-element granitic pegmatites. In: Černý, P. (Ed.), Granitic Pegmatites in Science and Industry. Mineralogical Association of Canada, Short Course Handbook 8, pp. 463–494.

Supplementary Files

This is a list of supplementary files associated with this preprint. Click to download.

- Suplemmant.docx